Copolymerization of Potassium Chloroacetate and Potassium *N*-Chloroacetyl-6-aminohexanoate

Sara Keiko Murase, Lourdes Franco, Alfonso Rodríguez-Galán, Jordi Puiggalí

Departament d'Enginyeria Química, Universitat Politècnica de Catalunya, Av. Diagonal 647, Barcelona E-08028, Spain

Received 26 June 2011; accepted 24 December 2011
DOI 10.1002/app.36708
Published online in Wiley Online Library (wileyonlinelibrary.com).

ABSTRACT: The polymerization kinetics of potassium chloroacetate (MGL), potassium *N*-chloroacetyl-6-aminohexanoate (MEA), and their mixtures was studied by Fourier transform infrared spectroscopy. The bulk polycondensation reaction was faster for MEA than for MGL but kinetic differences in the selected temperature range (110–130°C) were not large enough to make unfeasible copolymerization of both monomers. A decrease in the activation energy was deduced for the polycondensation of monomer mixtures with respect to that determined for the homopolymerization reaction of the predominant neat monomer. differential scanning calorimetry data also showed significant differences in the exothermic polycondensation peaks that suggested an effective copolymerization reaction and favored the kinetic process over the corresponding homopolymerization. The resulting new poly(ester amide)s were characterized by spectroscopy and thermal analysis. ^{1}H NMR spectra of samples with high MEA content revealed the existence of hetero-sequences whose ratio was slightly lower than that expected for a random polymerization of the two monomers. Samples with high molecular weights were only attained when the MGL molar ratio in the monomer mixture was lower than 65%. Calorimetric data showed that all samples were thermally stable and became amorphous for intermediate compositions. © 2012 Wiley Periodicals, Inc. J Appl Polym Sci 000: 000–000, 2012

Key words: biodegradable polymers; polyglycolide; poly(ester amide); polymerization kinetics; FTIR analysis

INTRODUCTION

Alkali halogenoacetates lead to polyglycolide (PGL) upon heating at temperatures higher than 100°C by a polycondensation reaction that has the formation of a metal halide salt as the driving force of the process. Thus, the reaction results in micrometer-sized metal halide crystals dispersed in a PGL matrix.[1] Polymerization rate and required reaction temperature are strongly dependent on the combination of halogen (e.g., Cl, Br, or I) and metal (e.g., Na, K, Rb, Cs, or Ag). Reaction can take place in the solid, liquid or a combination of both phases depending on the reaction temperature and the specific metal halide produced in the process. *In situ* experiments allowed verification of the phase at which the reaction proceeds. Techniques like X-ray spectroscopy (EXAFS),[2] X-ray diffraction,[2,3] infrared (IR) spectroscopy,[4] and small-angle X-ray scattering[5] were applied. In this way, a reaction of sodium chloroacetate was postulated to occur in the solid state with no detectable intermediate phases involved when the temperature was maintained between 120 and 140°C.[6] The reaction was found to proceed at a slow rate since a period of 1100 or 150 min was necessary to reach a complete conversion at temperatures of 140 or 160°C, respectively.[7]

Despite the advantages derived from the simplicity of this method, the low molecular weight that can be reached because of secondary reactions and thermal decomposition at the high temperatures required for the progress of the reaction hinders its application. This kind of solid-state reaction was also tested to obtain different polyesters [polylactide, poly(3-hydroxypropionate), and poly(2-hydroxybutyric acid)] with worse results than PGL in most cases.[8]

However, the method was successfully applied to obtain poly(ester amide)s (PEAs) constituted by an alternating sequence of glycolic acid and ω-amino acid units, whose synthesis was previously proposed on the basis of time-consuming methods involving selective protection and deprotection of reactive groups.[9] New monomers were easily synthesized, in this case, by the reaction of chloroacetyl chloride with the appropriated ω-amino acid and by subsequent neutralization with the selected metal hydroxide. This synthesis rendered high molecular weight samples when ω-amino acids had a high methylene

Correspondence to: J. Puiggalí (jordi.puiggali@upc.es).
Contract grant sponsors: MCYT/FEDER and AGAUR; contract grant numbers: MAT2009-11503, 2009SGR-1208.

content [i.e., 6-aminohexanoic (AH),[10] 11-aminoundecanoic,[11] and 12-aminododecanoic acid[12] derivatives]. Polymerizations could occur in the solid, liquid, or both phases, depending on the number of methylene groups and the kind of salt. In fact, these two conditioning factors have an influence on the melting point of the monomer, which can be either higher or lower than the reaction temperature.

Several studies were performed to determine the polymerization kinetics, thermal stability, and properties of these new PEAs.[12–14] Copolymerization of chloroacetate with *N*-chloroacetyl-ω-aminoalkanoates is also an interesting topic since it may render random copoly(ester amide)s with tunable properties as a result of the control over the ester/amide ratio.[15] This work specifically focuses on the copolymerization between a chloroacetate salt and the AH derivative. To favor copolymerization, the potassium chloroacetate (MGL) was selected because of the indicated low reactivity of the sodium salt, especially when compared with the AH derivative. The polymerization kinetics was evaluated by *in situ* Fourier transform infrared (FTIR) since it is sensitive to formation and destruction of chemical bonds. Calorimetric, thermogravimetric, chromatographic, and NMR spectroscopic techniques were applied to control polymerization and characterize the final reaction products. Hereafter, the two monomers will be named as MGL and potassium *N*-chloroacetyl-6-aminohexanoate (MEA) as they give rise to PGL and the alternating PEA constituted by glycolide and AH units. Monomer mixtures will be named indicating only the molar fraction of the MGL monomer (i.e., MGL-0.4 corresponds to the mixture with a 0.4 molar fraction of MGL), whereas samples derived from polymerization of a given mixture will be named by changing the first capital letter [i.e., P (polymer) instead of M (monomer)]. Thus, PGL-0.4 is for example the polymer obtained from the MGL-0.4 monomer mixture.

EXPERIMENTAL

Materials

Reagents and solvents for performing the synthesis shown in Figure 1 were purchased from Aldrich and used as received. 1,1,1,3,3,3-Hexafluoroisopropanol was purchased from Apollo Scientific with a 99% purity. *N*-Chloroacetyl-6-aminohexanoic acid was obtained as previously reported (Fig. 1).[10,11] MGL and MEA monomer salts were prepared by neutralization with KOH (1*M*) up to pH 10 or 12 of aqueous dilute solutions of chloroacetic acid and *N*-chloroacetyl-6-aminohexanoic acid, respectively. Water was subsequently removed by lyophilization. Monomer salt mixtures in the appropriate ratio were dissolved in methanol, keeping a total monomer concentration (i.e., MGL plus MEA) close to 0.02 mol/mL, and then lyophilized again. Finally, the recovered monomer mixture was kept at −20°C under vacuum to avoid further polymerization.

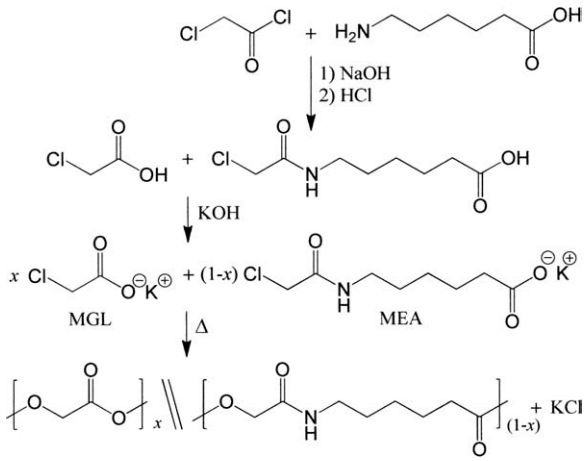

Figure 1 Synthesis scheme for the preparation of copolymers from mixtures of the potassium salts of chloroacetic acid and *N*-chloroacetyl-6-aminohexanoic acid.

Polymerization procedure

Polymerizations were carried out on a preparative scale by heating at selected temperatures the different mortared mixtures of potassium salts. Reactions were always carried out in a nitrogen atmosphere to avoid temperature-induced secondary reactions.

Mixtures with a MGL content equal or lower than 65% (i.e., from MGL-0 to MGL-0.65) liquefied during polymerization and consequently reaction was conducted in glass tubes provided with magnetic stirring to improve mixing. Polycondensation was first performed at low temperature in two steps at 115 and 120°C to favor heteropolymerization and then post-polymerized in an oven at 125°C for 2 h to ensure complete conversion. Polymerization of MGL-1 and MGL-0.8 samples occurred entirely in the solid state, and consequently sealed tubes were kept without stirring in an oven at a fixed selected temperature (i.e., 125°C). Reaction times for each step and sample will be later specified in the corresponding section.

After cooling, a white-brown solid was recovered, dissolved in formic acid and reprecipitated with water/methanol (1 : 1 *v*/*v*).

Measurements

Molecular weights and polydispersity index (PDI) were estimated by size exclusion chromatography using a liquid chromatograph (Shimadzu, model LC-8A) equipped with an Empower computer

program (Waters) and a refractive index detector (Shimadzu RID-10A). A PL HFIP gel guard precolumn and PL HFIP gel column (Agilent Technologies Deutschland GmbH) were employed. The column is characterized by a multipore technology with an efficiency > 30,000 p/m and a separation range between 500 and 1,000,000 g/mol. The polymer was dissolved and eluted in 1,1,1,3,3,3-hexafluoroisopropanol at a flow rate of 0.5 mL/min (injected volume 100 μL, sample concentration 1.5 mg/mL). The number and weight average molecular weights were calculated using polymethyl methacrylate standards, being the technical error of the measurement <10%.

IR absorption spectra were recorded with a Fourier transform FTIR 4100 Jasco spectrometer in the 4000–600 cm^{-1} range. A Specac model MKII Golden Gate attenuated total reflection (ATR) set-up with a heated Diamond ATR Top-Plate which can be used up to 200°C, and a Series 4000 high stability temperature controller were also utilized.

^1H NMR spectra were obtained with a Bruker AMX-300 spectrometer operating at 300.1 MHz. Chemical shifts were calibrated using tetramethylsilane as an internal standard. Deuterated trifluoroacetic acid/chloroform mixtures (3 : 1 *v*/*v*) were used as the solvent.

Calorimetric data were obtained by differential scanning calorimetry (DSC) with a TA Instruments Q100 series equipped with a refrigerated cooling system (RCS) which operates from −90°C to 550°C. Experiments were conducted under a flow of dry nitrogen with a sample weight of approximately 10 mg while calibration was performed with indium. Heating and cooling runs were carried out at a rate of 20°C/min.

Thermal degradation was studied at heating rates of 20 and 2°C/min with around 10 mg samples in a Q50 thermogravimetric analyzer of TA Instruments and under a flow of dry nitrogen. The analysis was performed in the 50–600°C temperature range.

RESULTS AND DISCUSSION

Thermogravimetric analysis of the polymerization process

Thermal stability of the two monomers and their mixtures was studied since bulk polymerizations are carried out at relatively high temperatures and for a long time. Figure 2(a) shows the TGA traces acquired at a heating rate of 20°C/min for all studied mixtures, whereas Table I summarizes the main decomposition data. Note that these curves could not be strictly associated with the decomposition of monomers since the polycondensation reaction took place during heating, and consequently the final traces should be similar to those of final copolymers.

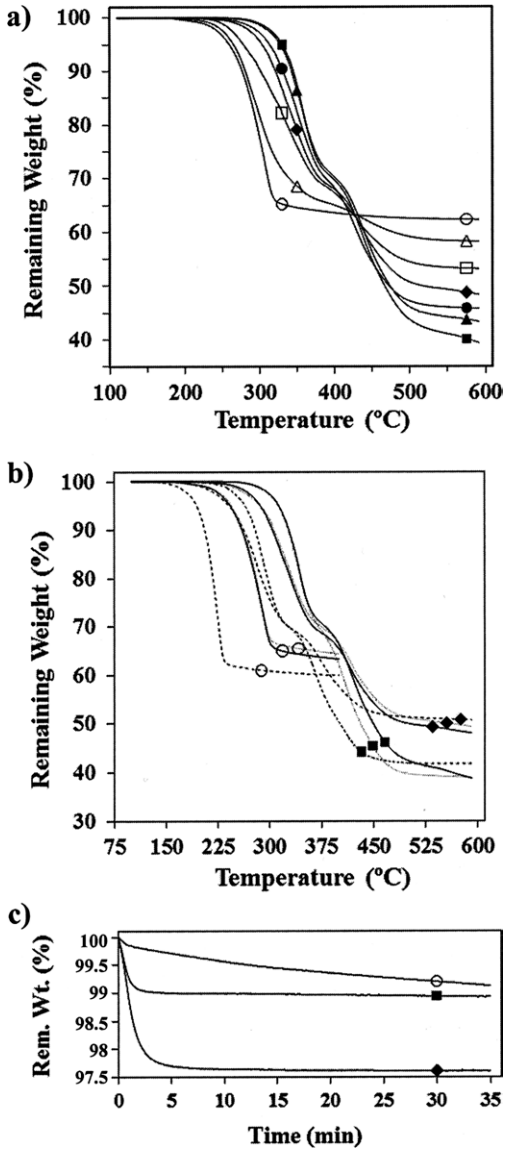

Figure 2 (a) Thermogravimetric curves (20°C/min) of mixtures of the two monomers with 1 (○), 0.8 (Δ), 0.65 (□), 0.5 (◆), 0.35 (●), 0.2 (▲), and 0 (■) molar fractions of MGL. (b) Thermogravimetric curves of mixtures of the two monomers with 1 (○), 0.5 (◆), and 0 (■) molar fractions of MGL. TGs were obtained at 20°C/min (solid lines), 2°C/min (dashed lines), and 20°C/min after keeping the sample at 130°C for 90–240 min (dotted lines). (c) Static thermogravimetric curves (120°C) of mixtures of the two monomers with 1 (○), 0.5 (◆), and 0 (■) molar fractions of MGL.

It is clear that the onset decomposition temperature decreased with the content of MGL and that mixtures with low MGL content appeared sufficiently stable to perform solid-state polymerizations at temperatures lower than 170°C (e.g., the onset temperature of the MGL-0.65 mixture was 187°C). Table I also reports the remaining weight at 600°C, which mainly corresponds to the KCl reaction byproduct. In all cases, the experimental remaining

TABLE I
Characteristic TGA Temperatures and Remaining Weight Percentages for the Decomposition of the Studied Monomer Mixtures

Sample	T_{onset} (°C)	$T_{10\%}$ (°C)	$T_{20\%}$ (°C)	$T_{40\%}$ (°C)	wt (%)
MGL-1	140	254	276	–	62
MGL-0.8	148	212	268	357	53
MGL-0.65	187	257	303	405	50
MGL-0.5	190	291	320	411	48
MGL-0.35	196	297	329	403	43
MGL-0.2	240	302	334	410	40
MGL-0	245	320	342	413	38

weights were slightly higher than those corresponding to the theoretical amount of salt (e.g., 56% and 30% for the MGL-1 and MGL-0 samples), indicating that organic char also formed under such experimental conditions. Curves show that MGL had a single decomposition step, whereas its mixtures with MEA had two steps, which should be assigned to the decomposition of glycolic acid and aminohexanoic acid units, as previously deduced in the degradation studies of the sequential copolymer constituted by the two indicated units.[14]

Figure 2(b) shows the influence of the heating rate on the thermal stability of monomers. As it is well known, a decreasing rate leads to a shift of the TG curves to a lower temperature (as shown for the heating traces obtained at 20 and 2°C/min). This should be considered for polymerizations performed at a fixed temperature. Figure 2(b) also contains the heating traces (20°C/min) of mixtures previously kept at 130°C for 240 min (MGL-0 and MGL-0.5) or 60 min (MGL-1), which should mainly correspond to the TG traces of the related copolymers due to the selected reaction conditions. It is highly interesting that significant differences exist for a given sample between the TG curve directly obtained from the monomer mixture and that obtained from the prepolymerized sample. Thus, the first decomposition step observed for the monomer mixtures shifts to higher temperatures when the sample is previously pre-polymerized at 130°C (i.e., MGL-0.5 sample). In this case, the remaining weight percentage at 600°C is in full agreement with the KCl content. This suggests that MGL can copolymerize at 130°C and render a more stable product. It therefore makes sense to undertake a careful study on the copolymerization process despite the slight thermal instability of the MGL monomer. Note also that the first decomposition step of MEA is not affected by the previous polymerization; in this case the second degradation step proceeds faster and the final constant weight percentage associated with KCl is attained at a lower temperature. Finally, Figure 2(b) clearly shows that the indicated stabilization effect does not exist when the single MGL monomer is considered.

Static thermogravimetries performed at 120°C [Fig. 2(c)] indicate that MGL has a slight but steady decomposition (i.e., it reaches 2.8% after 240 min; data not shown in the graph), in contrast with the constant percentage observed with MEA and monomer mixtures (e.g., MGL-0.5). These samples only revealed a slight initial weight decrease (3–4 min) associated with the water content. It must be noted that samples are highly hygroscopic and the water uptake strongly depends on their time of exposure to ambient conditions. Data suggest that, unlike the PEA monomer, neat MGL can easily undergo some degradation reactions that should lead to a low molecular weight.

Calorimetric data of the polymerization process

Figure 3 reports the different heating scans performed with the monomer mixtures. In all cases, only a single or several exothermic peaks indicative of polymerization processes were detected. Thus, polycondensation always started in the solid state since no melting endothermic peak was observed at temperatures lower than those corresponding to the above exotherms.

The DSC heating trace corresponding to MEA had two peaks (121 and 130°C). These suggested a complex reaction process where a first, quick condensation step occurred in the solid state between terminal groups which should be close enough in the crystalline structure for the reaction to take place. The second step could be associated with a slower condensation between reactive groups once a liquefied state was reached. In this case, molecular diffusion was necessary to approach these reactive

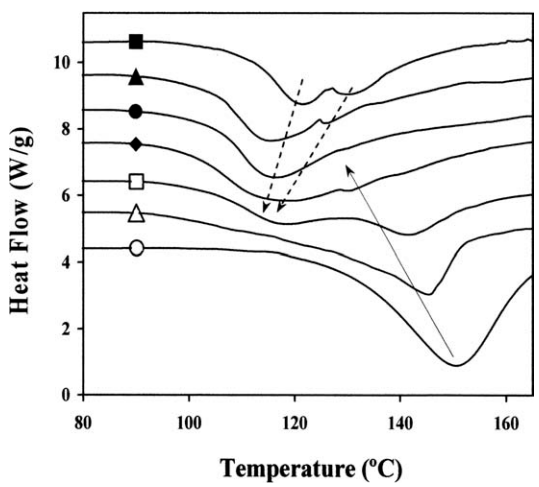

Figure 3 DSC heating runs (20°C/min) of mixtures of the two monomers with 1 (○), 0.8 (Δ), 0.65 (□), 0.5 (◆), 0.35 (●), 0.2 (▲), and 0 (■) molar fractions of MGL.

TABLE II
Calorimetric Polymerization Data for the Studied Monomer Mixtures

Sample	T (°C)	ΔH (J/g, kJ/mol)
MGL-1	151[a]	216, 28.6
MGL-0.8	146[a]	187, 29.0
MGL-0.65	119[b], 141[a]	174, 30.0
MGL-0.5	119[b], 130[a]	164, 31.1
MGL-0.35	116[b], 128[a]	152, 31.3
MGL-0.2	115[b], 126[b]	139, 31.1
MGL-0	121[b], 130[b]	137, 33.7

[a] Peaks associated to MGL rich phases.
[b] Peaks associated to MEA rich phases.

groups. By contrast, a single exotherm at a temperature of 151°C was observed for MGL, suggesting a single process occurring entirely in the solid state, as previously reported.[6]

Heating traces of monomer mixtures with high MEA content revealed that the two characteristic exothermic peaks shifted to lower temperatures and even converged to a single broad peak (see dashed arrows) with increasing the comonomer content. The shift of the exothermic peaks indicated that polymerization was favored when monomer mixtures were employed as will be confirmed later from the FTIR analyses. It should be pointed out that smaller and more imperfect crystals may be formed by evaporation of the aqueous solution of monomer salts and consequently the subsequent copolycondensation process may be enhanced.

DSC heating runs showed also that mixtures with high MGL content showed a single exothermic peak that also shifted to lower temperatures with increasing the comonomer ratio (see full arrow). Table II summarizes the observed exothermic peak temperatures and the global enthalpy, which was rather similar when referred to the molar salt content since, in all cases, the exothermic process corresponded to the formation of the same inorganic salt (KCl). This enthalpy logically increased with MGL content when referred to the sample weight.

FTIR kinetic analysis data of the polymerization process

A calorimetric kinetic analysis of the polymerization process is problematic since crystallization of poly(-glycolic acid-*alt*-6-aminohexanoic acid) rich sequences can also take place during isothermal polymerizations carried out at temperatures below 130°C (i.e., the polymer melting point is close to 156°C[11]). The occurrence of these endothermic/exothermic effects makes it difficult to evaluate the polymerization kinetics by DSC experiments. Thus, FTIR spectroscopy was considered as an ideal alternative technique given that the polymerization rate can be determined from the absorbance evolution of the newly formed bonds and those destroyed during polycondensation. Furthermore, some groups should also be sensitive to structural changes due to expected new intermolecular interactions.

Absorbance measurements of selected peaks during isothermal polymerizations were used to evaluate the relative conversion degree, $\alpha(t)$, for a given reaction time, t. The following equation was applied:

$$\alpha(t) = [A_t - A_0]/[A_\infty - A_0] \quad (1)$$

where A_t is the absorbance at time t, and A_∞ and A_0 are, respectively, the final and initial absorbances.

Figure 4(a) shows the main changes in the FTIR spectra occurring during polymerization of MGL. The C=O absorption band changed from 1600 to 1740 cm^{-1} as the salt carboxylate group reacted and gave rise to the ester bond. Hence, these bands progressively decreased and increased in intensity, respectively. Figure 5 compares the conversion calculated from the absorption data of the indicated bands at a polymerization temperature of 133°C. A similar sigmoid evolution is observed but the following kinetic analysis was performed considering only the most isolated 1740 cm^{-1} band.

The Avrami model[15,16] was used as a rough approximation to examine the polymerization kinetics, as previously applied for other similar systems. This rendered unnecessary a detailed study of the kinetic model.[11,17,18] Conversion was calculated by the following equation:

$$\alpha(t) = 1 - \exp[-Z(t - t_0)^n] \quad (2)$$

where Z and n are the corresponding Avrami parameters and t_0 the starting time of polymerization.

Plots of log $[-\ln(1 - \alpha(t))]$ vs. log (t) at different reaction temperatures gave straight lines with slopes corresponding to the Avrami exponent, n, and their intercepts at the origin to log Z. Moreover, a kinetic constant (k) with units independent of the Avrami exponent was calculated from $Z^{1/n}$. This parameter is summarized in Table III for the test temperatures in the range 120–165°C, together with half conversion times ($\tau_{1/2}$). These times could be easily estimated from the conversion curves, i.e., without assuming a specific kinetic model. As expected, the kinetic constant increased with the polymerization temperature and evolved similarly to the reciprocal of the half polymerization time, $1/\tau_{1/2}$, as shown in Figure 6. This good agreement is relevant since the Avrami analysis results are corroborated by direct experimental measurements, such as half polymerization times.

The activation energy for polymerization of MGL was derived by assuming an Arrhenius-type

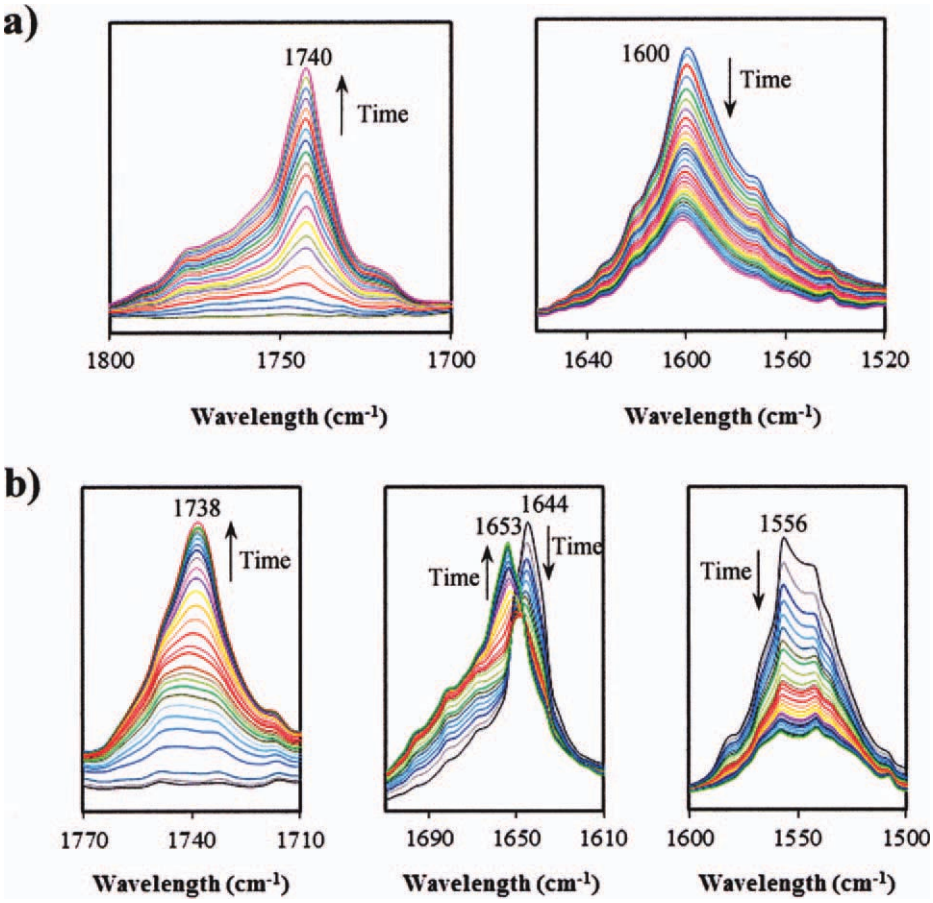

Figure 4 Evolution of representative absorption bands during polymerization of MGL (a) and MEA (b) at 165 and 130°C, respectively. [Color figure can be viewed in the online issue, which is available at wileyonlinelibrary.com.]

dependence of the kinetic constant on temperature, eq. (3), where E, A, and R are the activation energy, the preexponential frequency factor and the universal gas constant, respectively:

$$k = A \exp\left(-\frac{E}{RT}\right) \tag{3}$$

Plots of ln k vs. $1/T$ (Fig. 7) allowed the estimation of an activation energy of 69.4 kJ/mol.

Main changes in the FTIR spectra during polymerization of MEA are shown in Figure 4(b). In this case, the C=O absorption band changed from 1556 to 1738 cm^{-1} as the salt carboxylate group reacted and gave rise to the ester bond. The evolution of the band at 1556 cm^{-1} was more difficult to analyze due to the presence of a close amide II band. However, a similar time evolution for the representative bands at 1738 and 1556 cm^{-1} was found again, as shown in Figure 5. It is interesting to note that the amide I band moved from 1644 to 1653 cm^{-1} [Fig. 4(b)] during polymerization because of different hydrogen bond interactions in the monomer and polymer structures resulting from the presence of amide groups in both compounds. The kinetic analysis was performed using the 1738 cm^{-1} band only, as explained before for MGL. The kinetic parameters are summarized in Table III, whereas the temperature dependence of the kinetic constant and $1/\tau_{1/2}$ is

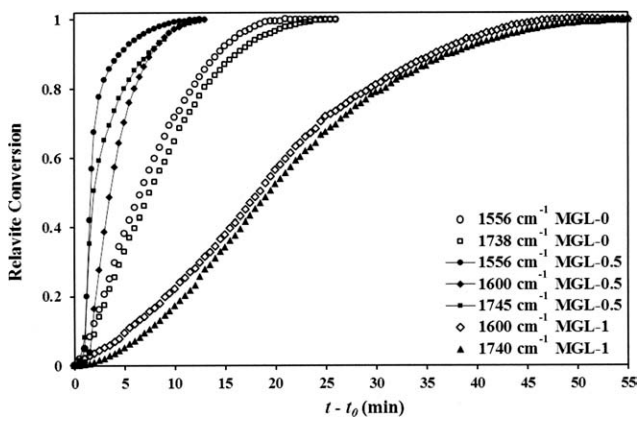

Figure 5 Plots of conversion deduced from the evolution of representative bands during isothermal polymerization of MGL at 133°C, MEA at 120°C and MGL-0.5 at 140°C. Temperatures have been selected to have well differentiated conversion curves for the three polymers but also for being close to the polymerization temperature employed in the synthesis at the preparative scale.

TABLE III
Kinetic Polymerization Data for the Studied Monomer Mixtures

Sample	T (°C)	$\tau_{1/2}$ (min)	k (min^{-1})	E_a (kJ/mol)	$A \cdot \times 10^{-6}$ (min^{-1})
MGL-0	100	20.0	0.020	75.5	833.38
	105	17.0	0.030		
	110	13.0	0.049		
	120	8.3	0.080		
	130	5.0	0.125		
MGL-0.2	95	17.5	0.031	65.5	63.27
	100	14.3	0.042		
	105	11.8	0.058		
	110	9.8	0.070		
	115	8.3	0.095		
MGL-0.35	100	11.3	0.058	57.9	7.17
	105	9.0	0.070		
	110	7.8	0.092		
	130	5.0	0.228		
MGL-0.5	95	12.0	0.050	57.5	7.08
	100	10.0	0.062		
	105	8.3	0.082		
	110	7.3	0.102		
MGL-0.8	130	15.8	0.033	66.0	11.83
	140	12.5	0.054		
	145	10.3	0.066		
	147	9.0	0.074		
	150	8.0	0.084		
MGL-1	123	22.3	0.020	69.4	29.09
	133	16.0	0.034		
	135	14.0	0.038		
	140	12.0	0.051		
	155	6.0	0.098		
	165	4.0	0.152		

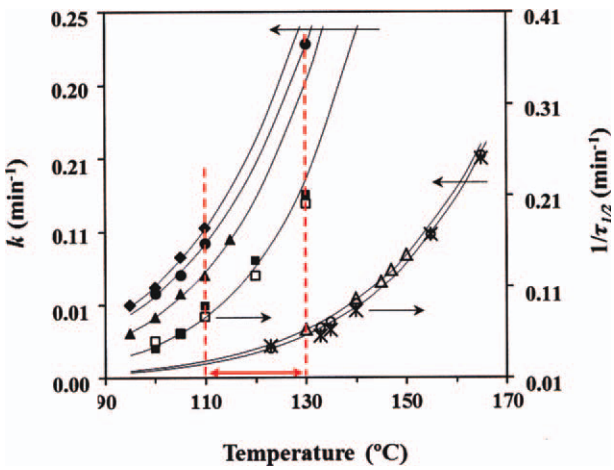

Figure 6 Temperature dependence of the kinetic polymerization constant (solid lines) for MGL-1 (○), MGL-0.8 (Δ), MGL-0.5 (◆), MGL-0.35 (●), MGL-0.2 (▲), and MGL-0 (■) monomer mixtures. For comparison purposes, the reciprocal of the half polymerization time determined at different isothermal polymerization temperatures for the MGL-1 (*) and MGL-0 (□) mixtures is also plotted. [Color figure can be viewed in the online issue, which is available at wileyonlinelibrary.com.]

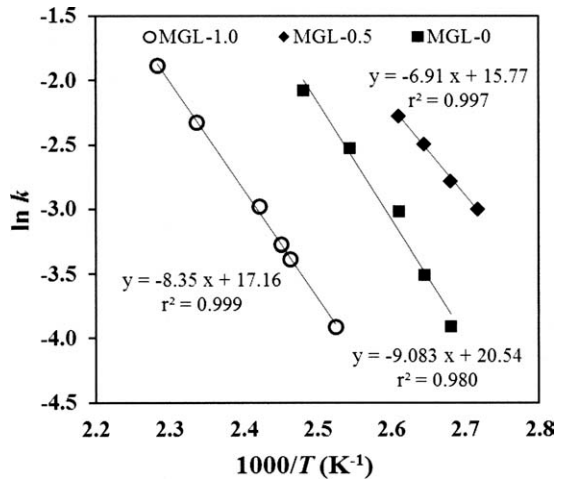

Figure 7 Plots of ln k vs. the reciprocal of the polymerization temperature for MGL-1 (○), MGL-0.5 (◆), and MGL-0 (■) monomer mixtures.

shown in Figure 6. It is clear that MEA polymerizes faster than MGL but differences are considered in an acceptable range for copolymerizations performed when at temperatures below 130°C. As can be seen in Figure 7 and Table III, MEA and MGL have similar activation energies (75.5 and 69.4 kJ/mol, respectively) but the preexponential frequency factor of the former is considerably higher ($833 \times 10^{+6}$ vs. $29 \times 10^{+6}$ min^{-1}), becoming the crucial parameter in explaining the observed polymerization rate difference.

The evolution of bands at 1740, 1600, 1556 cm^{-1} during polymerization of the monomer mixtures is significantly different, as shown in Figure 5 for the MGL-0.5 sample. Thus, the band at 1556 cm^{-1} changed faster than that at 1600 cm^{-1}, suggesting a higher polymerization rate for the MEA monomer, in agreement with the previous analysis and DSC calorimetric data. The evolution of the ester band at 1740 cm^{-1} extended over the time period when the absorption of the two COO^{-} carboxylate bands decreased, which is the result of the polymerization of either monomer. Therefore, the kinetic analysis of the overall polymerization process was conducted for all mixtures considering only the evolution of the 1740 cm^{-1} band. The time evolution of this kinetic constant is compared in Figure 6 and Table III for all studied samples, with the exception of MGL-0.65, which gave confusing results since at low polymerization temperature mainly involves the MEA monomer whereas at high temperature the contribution of MGL was highly significant. For the other samples, a single polymerization process became predominant, thereby allowing a kinetic analysis to be performed. Table III shows the deduced Arrhenius parameters and a decrease in the activation energy when MEA was mixed with MGL (e.g., 75.5 and

TABLE IV
Synthesis and Basic Characterization Data of PGL-*x* Copolymers

Sample	Temperature, time (°C, min)	Yield[a] (%)	M_w[b] (g/mol)	PDI[b]	G–G^*[c] (mol %)	HoS[d] (mol %)	T_g[e] (°C)	T_f[f] (°C)	ΔH_f[f] (J/g)
PGL-0[g]	115, 20; 120, 7	75	28,000	2.2	50–0	100, 100	15	157	75
PGL-0.2[g]	115, 16; 120, 5	65	26,000	2.2	52–7	78, 65	18	141	70
PGL-0.35[g]	115, 12; 120, 5	60	23,000	2.1	58–16	62, 46	18	119	20
PGL-0.5[g]	115, 12; 120, 5	54	20,000	2.0	59–34	31, 37	18	108[h]	11
PGL-0.65[g]	115, 35; 120, 8	49	18,000	2.1	72–45	55, 40	24	115	16
PGL-0.8	125, 180	40	15,000	2.1	77–70	49, 55	27	202	20
PGL-1	125, 240	30	12,000	2.2	100–100	100, 100	48	167, **202**	45

[a] After reprecipitation.
[b] Determined by GPC from reprecipitated samples.
[c] Total content of glycolic acid units (G) and of glycolic acid units (G^*) coming from polymerization of MGL as determined from ^{1}H NMR spectra [eqs. (4) and (5)]. Values correspond to reprecipitated samples.
[d] Percentage of homo-sequences determined from ^{1}H NMR spectra [eq. (6)] of as-synthesized samples (left) and calculated for a random distribution (right).
[e] Determined from the DSC heating scan of melt quenched reprecipitated samples.
[f] Determined from the DSC heating scan of the reprecipitated samples. Bold number indicates the temperature of the main peak.
[g] Samples were post-polymerized in an oven at 125°C for 2 h.
[h] Complex signal with small shoulders at lower temperature.

57.5 kJ/mol were determined for MGL-0 and MGL-0.5, respectively, as shown in Fig. 7). The preexponential factor also decreased gradually but this was clearly compensated by the decrease in the activation energy. In summary, the overall polymerization rate was enhanced when MEA was mixed with MGL, in agreement with DSC observations. The effect of the addition of MEA on the polymerization kinetics of MGL was less clear since data concerning MGL-1 and MGL-0.8 were similar, although a small increase was detected upon addition of MEA. Note that both the preexponential factor and the activation energy were slightly lower for MGL-0.8.

Characterization of PGL-*n* samples

Copolymerizations were performed at the lowest temperature that ensures the progress of reaction in a suitable time scale and minimizes the reactivity difference between the two involved monomers. Thus, MEA rich mixtures started to polymerize at 115°C and then the temperature was raised to 120°C. Selected temperatures and required reaction times are summarized in Table IV. A post-polymerization was finally carried out at 125°C for 2 h to improve the final molecular weight, although no terminal groups were detected in the FTIR spectra taken as a control after the reaction times. MGL rich mixtures (i.e., $x = 0.8$) were polymerized at 125°C in a single step that required a longer reaction time because of their lower reactivity and occurrence of polycondensation entirely in the solid state. Table IV illustrates how the reaction time for mixtures with $x < 0.8$ decreases with increasing MGL content, as expected also from the previous kinetic analysis.

Polymerization yields were obviously practically quantitative before performing reprecipitation. However, and as shown in Table IV, yields decreased gradually (i.e., from 75 to 30%) with the MGL content in the reaction mixture. This result can be justified by assuming that more soluble oligomers formed from MGL rich mixtures. In any case, results seem highly promising for mixtures with $x < 0.8$. GPC data (Table IV, Fig. 8) also pointed to a continuous decrease in the molecular weight with the MGL content in the reaction mixture, suggesting that soluble fractions should correspond to MGL rich oligomers.

Figure 9 shows the FTIR spectra of all synthesized samples where typical ester (C=O, $\sim$ 1740 cm^{-1};

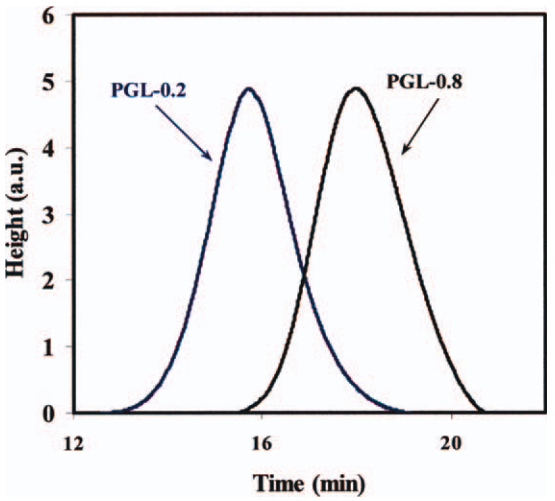

Figure 8 GPC chromatograms corresponding to the PGL-0.8 and PGL-0.20 representative copolymers. [Color figure can be viewed in the online issue, which is available at wileyonlinelibrary.com.]

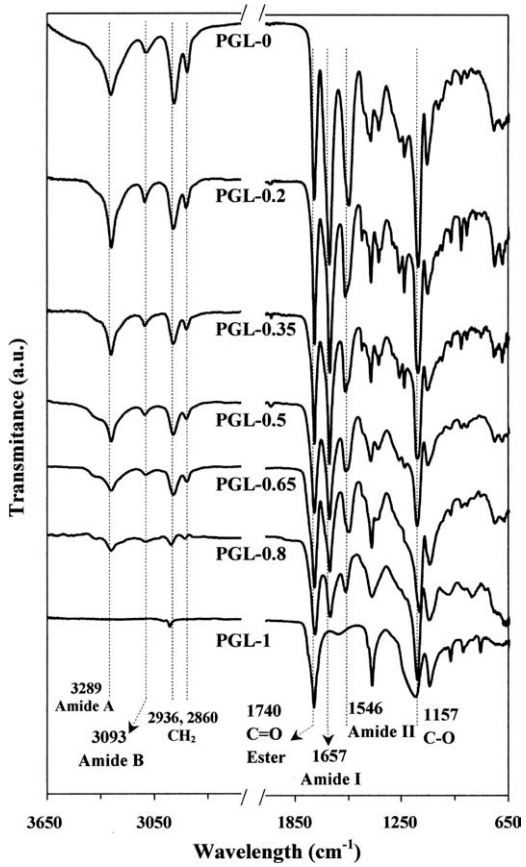

Figure 9 FTIR spectra of all PGL-*x* copolymers.

C—O, ~ 1157 cm^{-1}), amide (A, ~ 3289 cm^{-1}; B, ~ 3093 cm^{-1}; I, ~ 1657 cm^{-1}; II, ~ 1546 cm^{-1}), and methylene (2936 and 2860 cm^{-1}) bands were detected. Logically, the ratio between both ester and amide bands (e.g., between C=O and amide I bands) and ester and methylene bands gradually decreased with increasing MEA content. A small signal attributable to unreacted terminal groups (~ 1600 cm^{-1}) was observed in the PGL homopolymer only, as could be presumed from its low molecular weight.

Signals corresponding to the AH units were well distinguished in the ^{1}H NMR spectra (Fig. 10) and appeared insensitive to chemical sequences since the AH unit was always linked at each end to glycolic acid (G) units. Protons assigned to these G units gave rise to a complex signal in the 5.0–4.8 ppm range and additional peaks at 4.6–4.4 ppm corresponding to terminal units which were, as expected, more significant in MGL rich samples.

^{1}H NMR spectra allowed to determine for each sample the total molar content of G units and also the content of G units coming from the MGL monomer (denoted as G*) or the MEA monomer (denoted as G^+). Thus, the molar content of *G* and *G** units were determined for each sample by considering the global area of the signals in the 5.0–4.4 ppm range ($A_{5.0–4.4}$) and that of a representative AH signal (i.e., $A_{3.43}$):

$$G\ (\%) = 100 \times A_{5.0–4.4}/(A_{5.0–4.4} + A_{3.43}) \quad (4)$$

$$G^*\ (\%) = 100 \times (A_{5.0–4.4} - A_{3.43})/(A_{5.0–4.4} + A_{3.43}) \quad (5)$$

Logically, ratios determined for the as-synthesized samples were always in close agreement with the molar feed ratio. However, after reprecipitation MGL content decreased, suggesting again that soluble oligomeric fractions were mainly due to polymerization of MGL.

Analysis of the complex signal at 5.0–4.8 ppm is highly relevant since it allows collecting information of all chemical sequences obtained after copolymerization. Glycolic acid signals can be divided into those coming from the MEA monomer (i.e., G^+-AH sequence) and those coming from the MGL monomer, as summarized in Table V. The signal corresponding to G^+ units was split according to the previous monomer (i.e., MGL or MEA) and gave rise to signals at 4.92 ppm and 4.85 ppm, which corresponded to triads G*–$\mathbf{G}^+$–AH and AH–$\mathbf{G}^+$–AH, respectively. The latter triad is characteristic of the PEA homopolymer and appeared with great

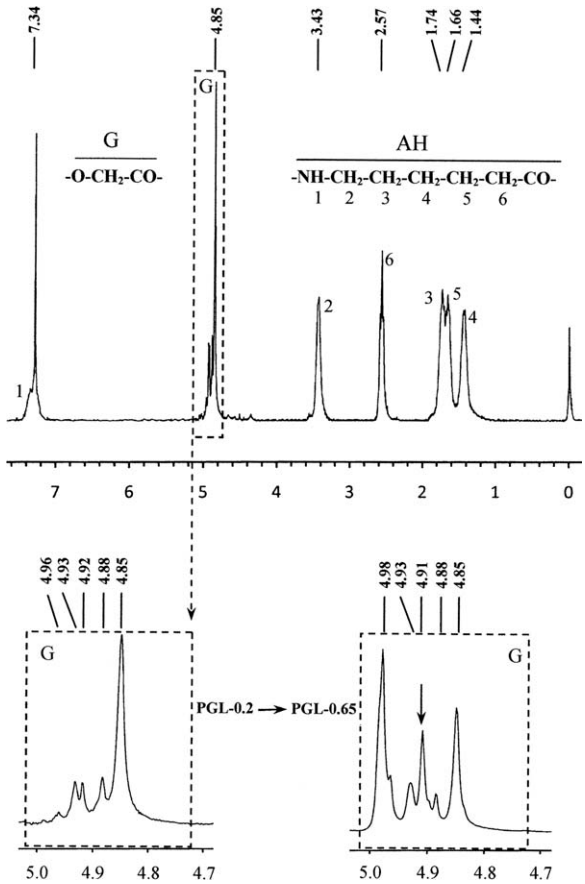

Figure 10 ^{1}H NMR spectrum of PGL-0.2 with assignment of main peaks. Insets show the region corresponding to the glycolide protons for PGL-0.2 and PGL-0.65 samples.

TABLE V
Assignment (δ, ppm) of Sequences Involving Peaks of the Glycolic Acid Units[a]

Monomer sequence	Unit sequence[b]	δ
MGL–**MGL**–MGL	G*–**G***–G*	4.98
MGL–**MGL**–MEA	G*–**G***–G^+–AH	4.93
MEA–**MGL**–MGL	AH–**G***–G*–G	4.93
MEA–**MGL**–MEA	AH–**G***–G^+–AH	4.88
MGL–**MEA**	G*–$\mathbf{G^+}$–AH	4.92
MEA–**MEA**	G^+–AH–$\mathbf{G^+}$–AH	4.85

[a] Signals corresponding to terminal groups are not indicated.
[b] G: Glycolic acid unit, G*: Glycolic acid unit coming from polymerization of MGL, G^+: Glycolic acid unit coming from polymerization of MEA, AH: Aminohexanoic acid unit.

intensity in copolymers prepared from MEA rich mixtures, as shown in Figure 10 inset, which illustrates the spectrum of the PGL-0.2 sample. Note also the great increase in the area of the peak at ca. 4.92 ppm (see arrow) with increasing MGL content in the monomer mixture.

Protons of G* units gave rise to three main signals that reflected the different possible combinations of monomers: MGL–MGL–MGL (4.98 ppm), MEA–MGL–MGL + MGL–MGL–MEA (4.93 ppm), and MEA–MGL–MEA (4.88 ppm). Note, for example, that the first sequence was insignificant or became predominant in the PGL-0.2 and PGL-0.65 samples, respectively. Again the area of this signal can be taken as an indication of the occurrence of homopolymerization reactions. In this way, a percentage of homo-sequences (HoS) could be calculated by eq. (6) if terminal group were not considered:

$$\text{HoS}\ (\%) = 100\ (A_{4.98} + A_{4.85})/(A_{5.0-4.8}) \qquad (6)$$

The values calculated for copolymers coming from MEA rich mixtures were always higher than those expected when a random copolymerization and the final copolymer composition {i.e., calculated as $100[x^3 + (1 - x)^2]$} were assumed. Thus, the higher reactivity of MEA led to predominant homo-sequences but carefully selected reaction conditions made it possible to obtain a large amount of hetero-sequences that even approached a random distribution. Results were less clear for copolymers derived from MGL rich mixtures since hetero-sequences were predominant in some cases (e.g., PGL-0.5 and PGL-0.8 samples). It should be pointed out that the analysis of these samples may have been disturbed because terminal group signals (4.6–4.4 ppm) were not considered and mainly corresponded to G*G* sequences, as inferred from the fact that the oligomeric fractions were predominantly derived from the MGL monomer.

All synthesized samples were semicrystalline and exhibited a complex thermal behavior according to their composition, as summarized in Table IV. Specifically, calorimetric analysis led to the following conclusions: (a) Melting peaks associated with each homopolymer phase (i.e., 157 and 202°C for PGL-0 and PGL-1, respectively) were observed depending on the composition. Each peak decreased gradually and shifted to a lower temperature when the comonomer content in the sample increased; (b) The copolymer with the intermediate composition (PGL-0.5) showed the broader melting peak which logically had the lowest enthalpy and melting temperature; (c) The glass transition temperature increased gradually with MGL content in the monomer mixture, as could be presumed from the higher stiffness of the glycolic acid units. It is also interesting to note that copolymers hardly crystallized from the melt state, and consequently the above features associated with the melting were deduced from the heating scan of reprecipitated samples. Hot and cold crystallizations were only detected in copolymers with low comonomer content, as shown in Figure 11 for the PGL-0.2 sample. In this case, hot crystallization was hardly observed at 69°C (i.e., with an undercooling

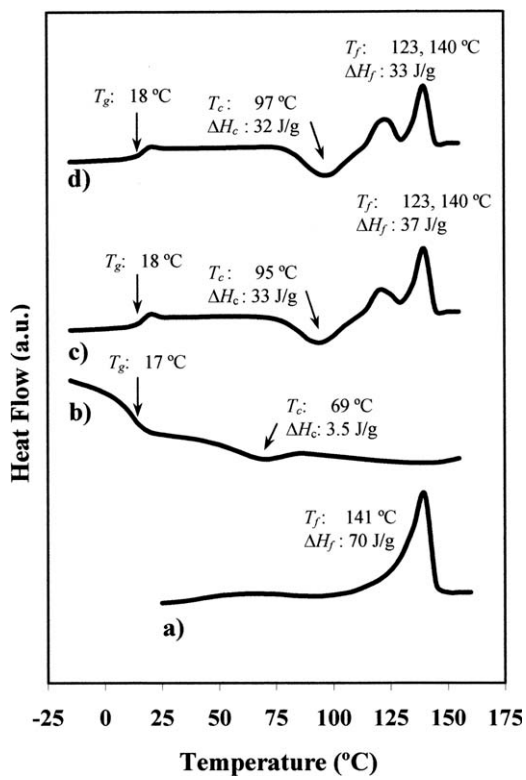

Figure 11 DSC traces showing the thermal treatment of a PGL-0.2 sample: (a) Heating run of the as-synthesized sample, (b) Cooling run from the melt state, (c) Heating run of a hot crystallized sample, and (d) Heating run of a sample quenched from the melt. The heat flow axis scale has been increased for the run (b) to show clearly the thermal transitions.

higher than 70°C), whereas cold crystallization occurred at a higher temperature (95–97°C) which favored the molecular ordering process. A double melting peak (123 and 140°C), which could be associated with the existence of lamellae of different thickness, was also observed in the heating run of both melt and quenched samples. Some defective/thinner lamellae seemed to form during cold crystallization and rendered the lowest melting peak (123°C) on heating.

Thermogravimetric traces of the synthesized samples (Fig. 12) were highly similar to those obtained from monomer mixtures [Fig. 2(a)] if it is taken into account that the removal of the inorganic salt led to a lower residual weight (Table VI). Some points are worth highlighting: (a) The onset degradation temperature (i.e., range between 225 and 245°C) was higher than the melting temperature in all cases, and consequently samples could be processed from the melt state. However, temperatures approached each other (i.e., the onset temperature decreased and the melting temperature increased) when samples had a high MGL content. Processing is still feasible but should be performed under well controlled conditions; (b) The organic char yield slightly increased with MGL content (13–18%) probably as a result of cross-linking reactions during degradation that mainly involved the glycolic acid units; (c) Degradation took place in two steps associated with the decomposition of glycolic acid (at the lower temperature) and aminohexanoic acid (at the higher temperature) units.

Degradation traces changed with the copolymer composition, and obviously the second step decreased gradually with increasing MGL content. The temperature associated at each step decreased with the MGL content in the monomer mixture (Table VI), indicating again that glycolide units enhanced the degradation process. (d) Significant differences were observed between DTGA curves of copolymers and the related monomer mixtures (Fig. 12). Peaks were better defined for copolymers and appeared at slightly higher temperatures. Decomposition was thus enhanced in the reaction mixture where furthermore a complex mechanism could be inferred from the multiple peaks observed in the first degradation step. In any case, it is clear that higher precautions should be taken into account for the polymerization process than for the polymer processing.

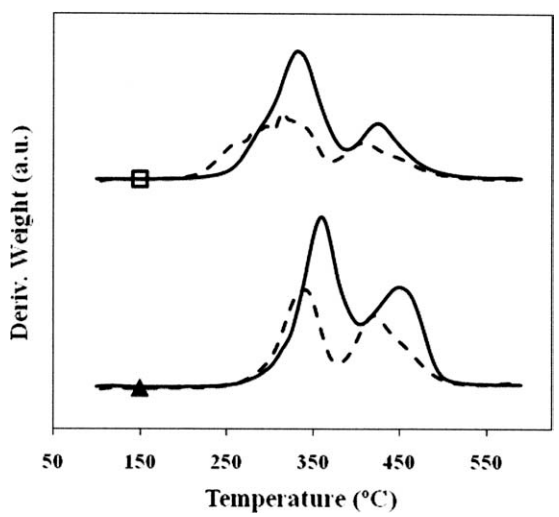

Figure 12 DTGA curves (20°C/min) of MGL-*x* (dashed lines) and PGL-*x* (full lines) samples. □ and ▲ denote samples with *x* equal to 0.65 and 0.20, respectively.

TABLE VI
Characteristic DTGA peak temperatures and remaining weight percentages for the decomposition of PGL-*x* samples[a]

Sample	T_1 (°C)	T_2 (°C)	wt (%)
PGL-0.65	332	425	18
PGL-0.5	341	433	19
PGL-0.35	340	437	16
PGL-0.2	360	451	15
PGL-0	382	460	13

[a] Data are reported only for samples which terminal groups are not so significant to influence on the decomposition process.

CONCLUSIONS

Copolymerization of MGL and MEA mixtures led to PEAs with a significant ratio of hetero-sequences when reaction conditions were conveniently chosen. FTIR analysis indicated higher reactivity for MEA but differences with MGL decreased with decreasing the polymerization temperature. Optimal conditions corresponded to the 110–130°C range since a temperature higher than a minimum value was also necessary to perform the polycondensation process in a suitable time scale.

In general, monomer mixtures showed lower activation energy than that found for the homopolymerization reaction of the predominant monomer. Thus, copolymers could be prepared under softer conditions than those used for the corresponding homopolymers.

Molecular weights and thermal stability decreased with the MGL content in the reaction mixture. However, copolymers with promising properties could be prepared when the MGL content was lower than 80%. These samples had melting temperatures ranging between 157 and 115°C and a variable melting enthalpy that depended on both composition and preparation process (i.e., recrystallization from dilute solutions, hot or cold crystallizations). A suite of compounds with variable crystallinity and ester/amide

ratio could thus be obtained by the new proposed synthesis and a series of PEAs based on glycolic acid units and having tunable degradability could be easily prepared with high yields.

S.K.M. acknowledges a FPI grant from MICINN.

References

1. Epple, M. J Mater Chem 1997, 7, 1037.
2. Epple, M.; Sazama, U.; Reller, A.; Hilbrandt, N.; Martin, M.; Tröger, L. Chem Commun 1996,1755.
3. Epple, M.; Kirschnick, H. Chem Ber 1996, 129, 1123.
4. Epple, M.; Kirschnick, H.; Thomas, J. M. J Therm Anal 1996, 47, 331.
5. Herzberg, O.; Gehrke, R.; Epple, M. Polymer 1999, 40, 507.
6. Aliev, A. E.; Elizabé, L.; Kariuki, B. M.; Kirschnick, H.; Thomas, J. M.; Epple, M.; Harris, K. D. M. Chem Eur J 2000, 6, 1120.
7. Schwarz, K.; Epple, M. Macromol Chem Phys 1999, 200, 2221.
8. Herzberg, O.; Epple, M. Eur J Inorg Chem 2001,1395.
9. Roby, M. S.; Jiang, Y.; U.S. Patent5,914,387, 22, June 1999.
10. Vera, M.; Rodríguez-Galán, A.; Puiggalí, J. Macromol Rapid Commun 2004, 25, 812.
11. Vera, M.; Franco, L.; Puiggalí, J. Macromol Chem Phys 2004, 205, 1782.
12. Botines, E.; Franco, L.; Ramis, X.; Puiggalí, J. J Polym Sci Part A: Polym Chem 2006, 44, 1199.
13. Ramis, X.; Salla, J. M.; Puiggalí, J. J Polym Sci Part A: Polym Chem 2005, 43, 1166.
14. Botines, E.; Franco, L.; Puiggalí, J. J Appl Polym Sci 2006, 102, 5545.
15. Avrami, M. J Chem Phys 1939, 7, 1103.
16. Avrami, M. J Chem Phys 1940, 8, 212.
17. Rodríguez-Galán, A.; Vera, M.; Jiménez, K.; Franco, L.; Puiggalí, J. Macromol Chem Phys 2003, 204, 2078.
18. Morales, L.; Franco, L.; Casas, M. T.; Puiggalí, J. J Polym Sci Part A: Polym Chem 2009, 47, 3616.